NATIONAL AERONAUTICS AND SPACE ADMINISTRATION

Technical Memorandum 33-504

Parametric Testing of an Externally Configured Thermionic Converter

K. Shimada

P. Rouklove

JET PROPULSION LABORATORY

CALIFORNIA INSTITUTE OF TECHNOLOGY

PASADENA, CALIFORNIA

November 1, 1971

NATIONAL AERONAUTICS AND SPACE ADMINISTRATION

Technical Memorandum 33-504

Parametric Testing of an Externally Configured Thermionic Converter

K. Shimada
P. Rouklove

JET PROPULSION LABORATORY
CALIFORNIA INSTITUTE OF TECHNOLOGY
PASADENA, CALIFORNIA

November 1, 1971

Prepared Under Contract No. NAS 7-100
National Aeronautics and Space Administration

PREFACE

The work described in this report was performed by the Guidance and Control Division under the Thermionic Reactor Systems Project of the Jet Propulsion Laboratory.

CONTENTS

FIGURES

ABSTRACT

A 25.4-cm-long externally configured converter was performance-tested at the Jet Propulsion Laboratory (JPL) by electrically heating the emitter to simulate reactor thermal power input. The measured maximum output power was limited by the maximum input power available from the electric RF induction heater. With maximum heater input power, the converter electric output was 178 W (1.95 W/cm^2) at an emitter temperature of 1946 K. This electric output power was smaller than expected. The power output during acceptance testing at the contractor's site was 5 W/cm^2 at 2000 K emitter temperature. The converter withstood 46 controlled shutdowns and 13 abrupt shutdowns without shorting and without loss of cesium.

A reactor-core-length (25.4-cm-long) cylindrical thermionic converter could be used as a full-length thermionic fuel element. Obtaining high output power and maintaining the emitter-to-collector gap without shorting are of major importance to the feasibility of a 25.4-cm-long reactor fuel element. The emitter of the converter is located externally to the collector to increase the fuel-volume fraction and to allow redundant collector cooling in a reactor configuration.

I. INTRODUCTION

The externally fueled converter concept offers advantages over the internally fueled converter concept for supplying electric power for outer planet electric propulsion missions. These advantages include: (1) one converter per thermionic fuel element, (2) a large fuel-volume fraction, (3) removal of electric connections, insulators, and metal-ceramic seals from the region of high neutron flux, (4) easy access for venting fission gases from the nuclear fuel, and (5) a redundant reactor cooling system. There are certain disadvantages, such as: (1) difficulties in maintaining the interelectrode space, (2) crack failures in the emitter body which would permit cesium to leak out and cause an open-circuit converter, and (3) difficulties in integrating the converters into a nuclear reactor configuration.

To help evaluate the externally fueled concept, a nonfueled (externally configured) thermionic converter was fabricated. The converter, designed and built by Thermo Electron Corporation (TECo), Waltham, Massachusetts, in accordance with JPL design requirements, was acceptance tested at TECo prior to delivery to JPL. Subsequently, the converter was tested parametrically at JPL for initial characterization prior to life testing.

During the parametric tests, the converter was electrically heated by an induction heater. The thermionic converter's static characteristics, dynamic characteristics, and other operational characteristics that are unique to this converter were investigated.

II. EXTERNALLY CONFIGURED CONVERTER DESIGN

As described in Ref. 1, the 25.4-cm-long emitter was fabricated from a cylinder of chemically vapor deposited tungsten hexafluoride, with an inner diameter of 1.143 cm and an outer diameter of 2.03 cm. The inner surface, which is the electron-emitting area of the emitter, had a total area of 91.2 cm^2. This surface was treated by electroetching for 15 minutes in sodium hydroxide and potassium ferrocyanide to remove all traces of impurities. Each end of the cylindrical emitter has an emitter sleeve 0.10 cm thick which acts as an emitter heat choke and an emitter power lead. The emitter leads are electron beam welded and brazed to niobium flanges which are both electrical output leads and mechanical supports. An alumina ring is embedded in each niobium flange to assist in maintaining the concentricity of the interelectrode spacing between emitter and the collector (Fig. 1).

The collector is made of a niobium 1% zirconium tubing with an inner diameter of 0.635 cm and an outer diameter of 1.092 cm. A molybdenum layer, a few microns thick, was deposited from a molybdenum filament on the active surface of the collector to improve performance. Embedded in the collector are three yttria-stabilized zirconia inserts, held with rhenium wires. The purpose of the inserts was to reduce the possibility of an emitter-to-collector contact, which could result from the thermally induced stresses.

Niobium flanges, brazed on each end of the collector, were welded to the metal-to-ceramic seal assemblies. The brazed Al_2O_3 seals were attached to the emitter flanges through niobium bellows. The bellows compensated for the differential expansion between the emitter and the collector. A "bird cage"-shaped collector-lead assembly was brazed to each collector flange to act as a flexible electrical lead and as a mechanical support. In addition, trim heaters were attached to the collector leads to further reduce heat losses to the water-cooled power leads.

The collector was cooled by water flowing through a stainless steel tube concentric to the inner cavity of the collector and separated from the collector inner wall by a gas gap (0.018 cm wide) maintained with a tantalum wire helix. A mixture of argon and helium was used in this gap to vary thermal conductance. The cesium reservoir, of the nonspillable type,

loaded with approximately 1 gram of cesium, was connected at the upper end of the converter. The cesium vapor pressure in the converter was varied through the use of a heater brazed onto the cesium reservoir. A cooling copper strap was also connected to provide a wide range of reservoir temperature.

The converter was connected to four disk-shaped copper electrodes, two on each end, acting as emitter and collector power leads. The water inlet and outlet tubings acted simultaneously as output power leads and cooling lines (Fig. 2).

III. TEST EQUIPMENT

During the laboratory test, an RF induction heater was used to heat the emitter. Five layers of tungsten foil were tightly wrapped around the emitter body to act as a radiation shield. The tungsten foils were perforated in five places corresponding to the locations of five blackbody holes drilled in the emitter body. However, only two blackbody holes were visible for the pyrometer measurements of the emitter temperature because the foils slipped during the initial heating.

The induction heater used in the tests was a Lepel dual-frequency 20-kVA RF generator (Fig. 3). The power output of this device was known to be marginal to operate this converter to full power, but no other equipment was available for the test. A coaxial RF feedthrough in the base plate of the bell jar was at a ground potential to reduce the RF radiations and to ensure personnel safety. The maximum power rating of the RF generator tube is 17.5 kW (10 kV, 1.75 A) for short-term operation; however, it was limited to 15 kW (10 kV, 1.5 A) for "safe" long-term operation. At this 15-kW power level, an estimated RF output power of 10 kW was available at the RF terminals of the generator. With a coupling coefficient estimated at 0.7, the maximum input power to the converter was about 7 kW.

The converter was vertically supported in a gantry bolted to the stainless steel base plate of the vacuum chamber (Fig. 2). This assembly consisted of six evenly spaced stainless steel rods, three of which were fixed to the copper electrodes used for the collector power leads and three for the emitter. Threaded alumina insulators at the center and the bottom of the rods were used to electrically insulate the collector and emitter from one another and from the base plate.

The bell jar was pumped by the vacuum system consisting of a 15.24-cm oil diffusion pump with liquid nitrogen baffle and a high-vacuum gate valve. The diffusion pump was connected to a 1400 liter/min roughing pump. This combination was selected over the normally preferred Vac-Ion[1] pump system, since the initial outgassing of the device and gantry was

[1] Varian Associates, Vacuum Division, Palo Alto, Calif.

expected to be considerably beyond the pumping capacity of available Vac-Ion pumps.

The base plate had a sufficient number of penetrations to provide feed-throughs for the instrumentation and for the water inlets and outlets used for cooling. The RF power was admitted to the bell jar through a 10-kW coaxial feed-through to eliminate overheating of the base plate by eddy current. The continuously flowing helium-argon gas mixture was admitted through a set of calibrated flow meters and a mixture plenum into the collector cooling gas gap, which was open to air at the outlet.

IV. CONVERTER CONTROLS AND DATA SYSTEM

With the data system, the following converter parameters were monitored and recorded: collector temperatures at both ends of the collector power take-off lead, cesium reservoir temperature, collector water cooling temperatures at the inlet and outlet for calorimetry, collector-lead heater power inputs, converter voltage output, converter total current output, individual emitter-lead current, dynamic-sweep current and voltage, vacuum pressure, running time, and pressures and flow rates of gas and water. The emitter temperature was measured with an optical pyrometer; other temperatures were measured with thermocouples referred to a 338.71 K (150°F) cold-junction reference. The bell jar, for safety reasons, was cooled by an array of six blowers. The provision for an individual measurement of the current from both ends of the emitter was very useful as it enabled the estimate of thermal distribution throughout the converter.

The converter outputs were monitored on four mirror-scale meters and measured with a six-digit digital voltmeter (Fig. 3). Since extremely large output current was expected, a bucking-voltage type of load was selected. This load consisted of a 1500-A, 5-V adjustable dc power supply driving the converter through a size 4/0 power cable. The input was 3-phase ac and adjustable through a ganged Variac[2] connected to a 3-phase output transformer. The output from the transformer, rectified by a 3-phase full-wave solid state rectifier, has a 4.2%, 360-Hz ripple. A transformer (5 V, 1000 A) driven from another Variac, was connected in series with the dc power supply to observe the dynamic characteristics of the converter on an oscilloscope. This was achieved by superposing a 60-Hz signal on the selected dc operating point of the I-V characteristics.

The collector trim heaters were operated from two Variac-controlled 12-V, 30-A power supplies. The cesium reservoir heater was controlled using an automatic temperature controller of the proportional type that maintained cesium reservoir temperature within ±2 K of the selected value.

[2]General Radio Co., West Concord, Mass.

Because of the uniquenesses in construction and operation of this converter, special safety measures were taken for the protection of personnel and of the equipment. The circuitry for preventing the converter from being damaged consisted of:

(1) A vacuum-activated device to prevent the converter from heating at a bell jar pressure above 6×10^{-2} N/m^2.

(2) Circuits to deactivate the induction heater when the cooling water flow to the system was insufficient.

(3) A valve that bypasses the water flow regulator and applies the full water line pressure into the cooling tubulation through the collector. This arrangement is to protect the converter from short-term overheating due to boiling of the collector cooling water. It was expected that full water line pressure would reestablish the water flow if nucleate boiling occurred. However, it was discovered that this valve, which was actuated by the water temperature transducer located at the collector outlet, was too slow to react as an efficient protection of the converter. During testing of an alternate protection method, the cooling water line plugged with mineral deposits and stopped all water flow. A demineralized water will be used for future tests.

V. PARAMETRIC TESTS

During the initial phase of the converter evaluation, the converter was tested for: (1) static power output, (2) temperature distributions along the emitter, and (3) dynamic volt-ampere characteristics. These tests determined the converter characteristics and the operating parameters for the life test.

A. Static Power Output

Static volt-ampere curves were obtained to determine the maximum output power of this converter under conditions of a constant input or a constant emitter temperature. The test circuit used during the parametric tests is schematically shown in Fig. 4.

The output current of the converter was varied by adjusting the dc supply voltage and dissipating the power into an air-cooled power cable (size 4/0) which was approximately 8 m long. The emitter temperature was measured by an optical pyrometer at one of the two blackbody holes located near the center of the emitter; the temperature measurements at other locations will be discussed separately in the following section.

The collector temperature was varied by adjusting the flow rate of the gas, mainly the helium, through a gas gap of 0.18 mm, while maintaining the flow rate of the water approximately 1 liter/min at 32 N/cm^2 water pressure. An arrangement for the precise calibration of flow rate was also provided. The water temperatures were measured at the inlet and the outlet for calorimetry purposes, and the collector temperature was monitored with a chromel-alumel thermocouple fastened on a collector lead at the converter. The average collector temperature was also determined from the thermal expansion of the niobium collector, which was measured by a cathetometer. The cesium reservoir temperature, which was varied by means of a cesium heater, was maintained constant within ±2 K of the preset value with an electronic controller.

The output current of the converter was measured at two emitter leads with two 750-A current shunts and at the common lead with a 1500-A current shunt. The output voltage of the converter was measured with a pair of tantalum potential leads attached to the emitter and collector leads on one

end of the converter. Although the output voltage was not measured at the other end of the converter, the difference between the two values was less than 0.01 V according to the independent voltage measurements. The difference would be larger if the currents from two emitters were not balanced.

As discussed earlier, the emitter of the converter, which was external to the collector, was heated from an induction generator rated at 20 kVA input (Fig. 5). The radio-frequency power at a frequency of approximately 400 kHz was coupled to the emitter from a 31-turn water-cooled copper coil closely wound around the emitter. The maximum power coupled to the converter was insufficient to bring the emitter temperature to 2000 K and the maximum emitter temperature attained was 1946 K.

A static volt-ampere curve for T_E = 1743 K, shown in Fig. 6, was obtained by optimizing temperatures of the cesium reservoir and the collector at output voltages of 0.2, 0.4, 0.6, and 0.8 V. The output power at the emitter temperature of 1743 K was 100.5 W, occurring at 0.4 V.

The maximum power achieved during the entire test was 178.3 W (1.95 W/cm^2) occurring at 0.48 V output with an emitter temperature of 1946 K; the cesium reservoir temperature was 633 K, and the average collector temperature was 900 K, which was determined from the measured elongation of the collector. The water calorimeter through the collector showed a temperature difference of 47.5 K at a flow rate of 0.802 liter/min. Therefore, the thermal power removed from the collector was 3.05 kW, and the conversion efficiency at the electrodes was 5.5%.

In this calculation, the total input power W_T to the converter is given by

$$W_T = W_C + W_E + W_O + W_S \tag{1}$$

where W_C is the heat removed from the collector, W_O the output power, W_E the heat reradiation from the external emitter to the bell jar, and W_S the other losses including conduction through output leads. The reradiation loss W_E occurs at the temperature of the tungsten foil which is wrapped around the emitter for a radiation shielding. The value of W_E is estimated to be 3.03 kW by assuming the surface temperature at 1700 K where the radiation power density was approximately 14 W/cm^2 and the total radiation area was

216 cm^2. Additional lead losses W_S are estimated at 10% of $W_C + W_E + W_O$; hence

$$W_S = 0.1 \cdot (W_C + W_E + W_O)$$

$$= 0.1 \cdot (3.05 + 3.03 + 0.178)$$

$$= 0.626. \quad (2)$$

Therefore, the total input power is given by

$$W_T = 3.05 + 3.03 + 0.178 + 0.626.$$

$$= 6.88. \quad (3)$$

Thus, the total input power coupled to the converter equals 6.88 kW, and, therefore, the coupling coefficient of RF power to the converter was approximately 70% at an RF input of 10 kW. Note, however that there would be no power lost by reradiation in a reactor operation since the emitter sees the fuel that is at a higher temperature than the emitter temperature.

The results at T_E = 1946 K are summarized below:

RF input	10 kW
RF power coupled to the converter, W_T	6.88 kW
W_T less the reradiation losses	3.85 kW
3.85 kW less the lead losses	3.23 kW
Converter output voltage	0.48 V
Converter output current	370.8 A
Output power	178 W
Power density at 91.2 cm^2	1.95 W/cm^2
Conversion efficiency (0.178 kW/3.23 kW × 100)	5.5%
Cesium reservoir temperature, T_R	633 K

Emitter temperature, T_E	1946 K (T_E/T_R = 3.07)
Collector temperature, T_C	900 K (T_C/T_R = 1.42)

Other characteristics which require special attention during the converter operation are listed below:

(1) The converter output is sensitive to the helium gas flow, but not to the argon gas. The output is also sensitive to the direction of gas flow.

(2) Excessive cooling of the collector and insufficient heating of the collector current leads results in the formation of a parasitic reservoir for cesium.

(3) The final output of the converter is sensitive to the adjustment of cesium and gas controls; however, the response time is long, i. e., 10 to 30 min. Therefore, a small adjustment frequently results in over- or under-shoot in the output.

The variations of the output power with the output voltage are compared in Fig. 7 for the cases with constant emitter temperature and with constant input power. The results show that the output power does not vary more than ±5% for output voltages between 0. 4 and 1. 0 V as long as the input power remains constant. This behavior was expected from the self-adjustment of the emitter temperature (Ref. 2) that occurred with the constant input power operation.

To evaluate the temperature drop across the thickness of the emitter, the emitter surface temperature T_E was calculated from the emitter blackbody hole temperature T_B for a given thermal heat flux. With the geometry shown in Fig. 8, one obtains

$$dT = \frac{Q}{\sigma \cdot 2\pi r}\, dr \tag{4}$$

where dT is the temperature drop across a dr cm thick emitter at radius r, σ is the thermal conductivity of tungsten (1.06 W/K-cm), and Q is the heat flux per unit length of the emitter at r. Since

$$Q = 2\pi \cdot 0.5715 \cdot q_1 \tag{5}$$

where q_1 is the heat flux density at the emitter surface (r = 0.5715 cm), one obtains

$$dT = \frac{2\pi \times 0.5715\, q_1}{2\pi \times 1.06\, r}\, dr$$

$$= 0.539\, q_1 \frac{dr}{r}. \tag{6}$$

Therefore, the total temperature drop ΔT between the bottom of the blackbody hole and the emitter surface is given by

$$\Delta T = 0.539\, q_1 \ln \frac{0.673}{0.5715}$$

$$= 0.0882\, q_1 . \tag{7}$$

At T_E = 1946 K, calculated ΔT equals 3.1 K. Therefore, the temperature correction required to convert from the blackbody temperature T_B to the emitter surface temperature T_E is within an experimental error, and T_B can be considered equal to T_E for all practical purposes.

B. Emitter Temperature Distribution

The effects of the temperature distribution along the emitter on the power output were investigated experimentally. The distribution of the temperature was measured at two blackbody holes and four surfaces by an optical pyrometer. By assuming a symmetrical temperature distribution about the center of the emitter and applying the experimental temperature corrections to obtain an equivalent blackbody temperature for four surfaces, temperature distributions such as those shown in Fig. 9 were obtained.

The distribution labeled No. 1 was obtained by spacing the induction coil, having a total of 31 turns, evenly (0.84 cm/turn) between two ends of the emitter. The distribution No. 2 was obtained by making smaller pitches for approximately 10 turns at both ends of the coil. The second case resulted in a more uniform temperature of $1860\ ^{+0}_{-60}$ K, whereas the first case resulted in the temperature of $1860\ ^{+20}_{-130}$ K. The corresponding output power was 161.7 W at 0.507 V for the more uniform temperature No. 2 and 122.6 W at 0.427 V for the No. 1 case. The result showed that the uniform temperature along the emitter produced a larger output power for the same average emitter temperature. In the example shown in curve No. 1, a total of 50% (25% at each end) of the converter was operating at emitter temperatures that are lower than that in the center by as much as 100 K. Therefore, the output power from the low-temperature zone could have been 1/2 of that from the center; thus the total output power was approximately 3/4 of the value with a uniform temperature. The incentive for power flattening the reactor, in which these converters are to operate, is evident from these results.

C. Dynamic Volt-Ampere Characteristics

Dynamic volt-ampere curves were obtained on an oscilloscope by activating the 60-Hz sweep transformer (5-V, 1000-A ac) shown in Fig. 4. During the measurements, the converter was first stabilized at a preselected dc operating point and then the sweep voltage was increased manually for approximately 5 s to record a volt-ampere curve. Although the thermal inertia of the converter was large, a reduction of the output current was noticeable because of increased electron cooling when the sweep voltage was increased. Typical dynamic curves at four different emitter temperatures are shown in Fig. 10. In the original oscillogram, there were traces of ringing originating in the filter that was used to reduce the RF noise levels below 10 mV. The ringing is a transient associated with the output levels of the induction heater, which pulsates at a rate of 360 Hz.

All thermocouple wires and potential leads were electrostatically shielded to reduce the interference from RF power. The shielding was effective enough to permit the acquisition of static data with a digital voltmeter having a good common-mode rejection. A set of dynamic volt-ampere curves taken at a constant emitter temperature of 1910 K with cesium temperatures

between 565 and 616 K are shown in Fig. 11. An inflexion point on the volt-ampere curve that is easily recognizable in converters having plane-parallel electrode geometry was obscured considerably in this converter. The non-uniformity of the emitter temperature was likely to have been the cause.

During the measurements described above, the induction heater having a 20-kVA input rating was deliberately overloaded to achieve emitter temperatures above 1850 K. To avoid the need for such undesirable overloading in future tests, the reradiation from the externally configured emitter must be reduced. For this purpose, 0.32-cm-thick zirconia felt (ZIRCAR) was fitted inside the RF coil around the converter. Although this arrangement appeared effective, undesirable RF electrical breakdowns occurred numerous times over and through the felt. When a sustained arcing occurred, the felt melted at localized spots. The arcing was caused partially by the burst of gas from the felt and partially by the conduction across the felt surface. It is also possible that a chemical reaction occurred between the zirconia and the asbestos cord used in holding the ZIRCAR. Such a reaction could have changed the electrical properties of the material.

Further tests of the converter were interrupted prematurely because of plugging in the collector cooling water line. The plugging occurred in the nickel tubing (0.25-cm ID) as well as the stainless steel tubing (0.41-cm ID) used for cooling the collector. Nucleate boiling, which results in the formation of large water vapor bubbles, occurred in the cooling water line, especially at a joint between the nickel and stainless steel tubing having two different diameters, and the subsequent plugging occurred.

Also, the need for a distilled, demineralized water and completely dry gases for the gas gap was indicated for future tests.

VI. CONCLUSION

Parametric tests of an externally configured converter were performed to evaluate its power output and operational characteristics. The maximum output power, which was limited by the input power of an available induction heater, was 178 W (1.95 W/cm^2) at an emitter temperature of 1946 K. The conversion efficiency calculated from the calorimetry was 5.5%.

The importance of the emitter temperature flattening to achieve high performance was clearly indicated. The reduction in output power is as large as 25% when the temperature distribution is $1860\ ^{+20}_{-130}$ K instead of $1860\ ^{+0}_{-60}$ K.

Other operational characteristics are: (1) slow response of converter output to changes in cesium pressure and collector temperature, (2) an occasional appearance of a hysteresis in the output, which could be caused by different temperature profiles along the emitter for an identical temperature at one point, (3) difficulties due to the heating arrangement using an induction heater whose RF power output could not be adjusted smoothly, and (4) requirements for an extra filtering to reduce RF interference with measurements.

Although the plugging of the water line caused the premature termination of the test after 190 h, the converter itself maintained its integrity and withstood 46 controlled shutdowns and approximately 13 abrupt shutdowns by RF electrical breakdowns and input power outages.

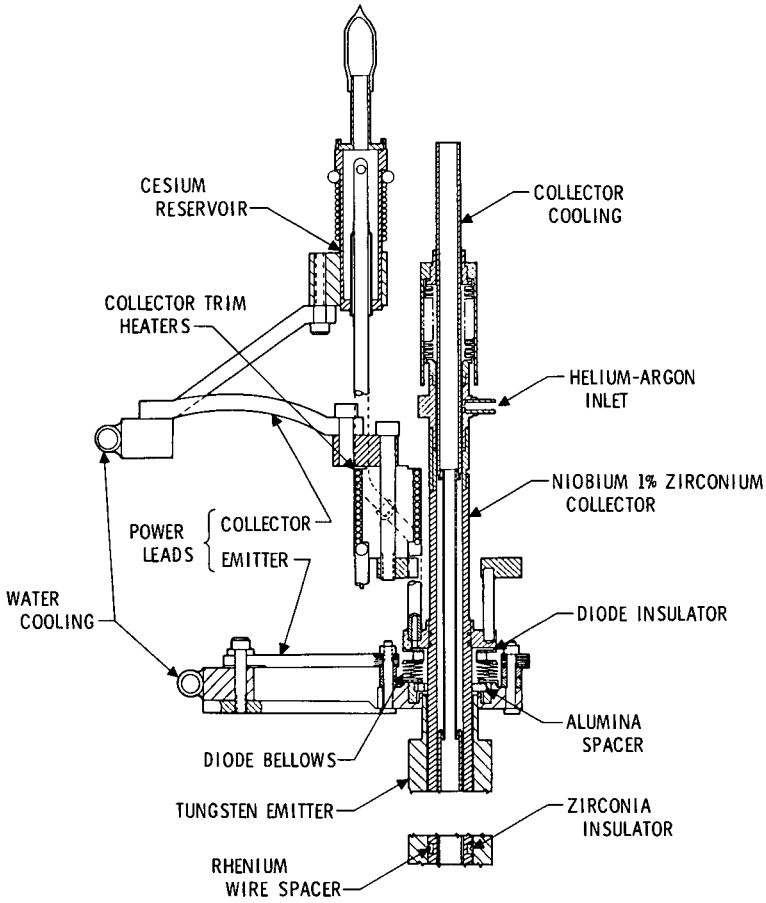

Fig. 1. Schematic diagram of converter, cesium-reservoir end

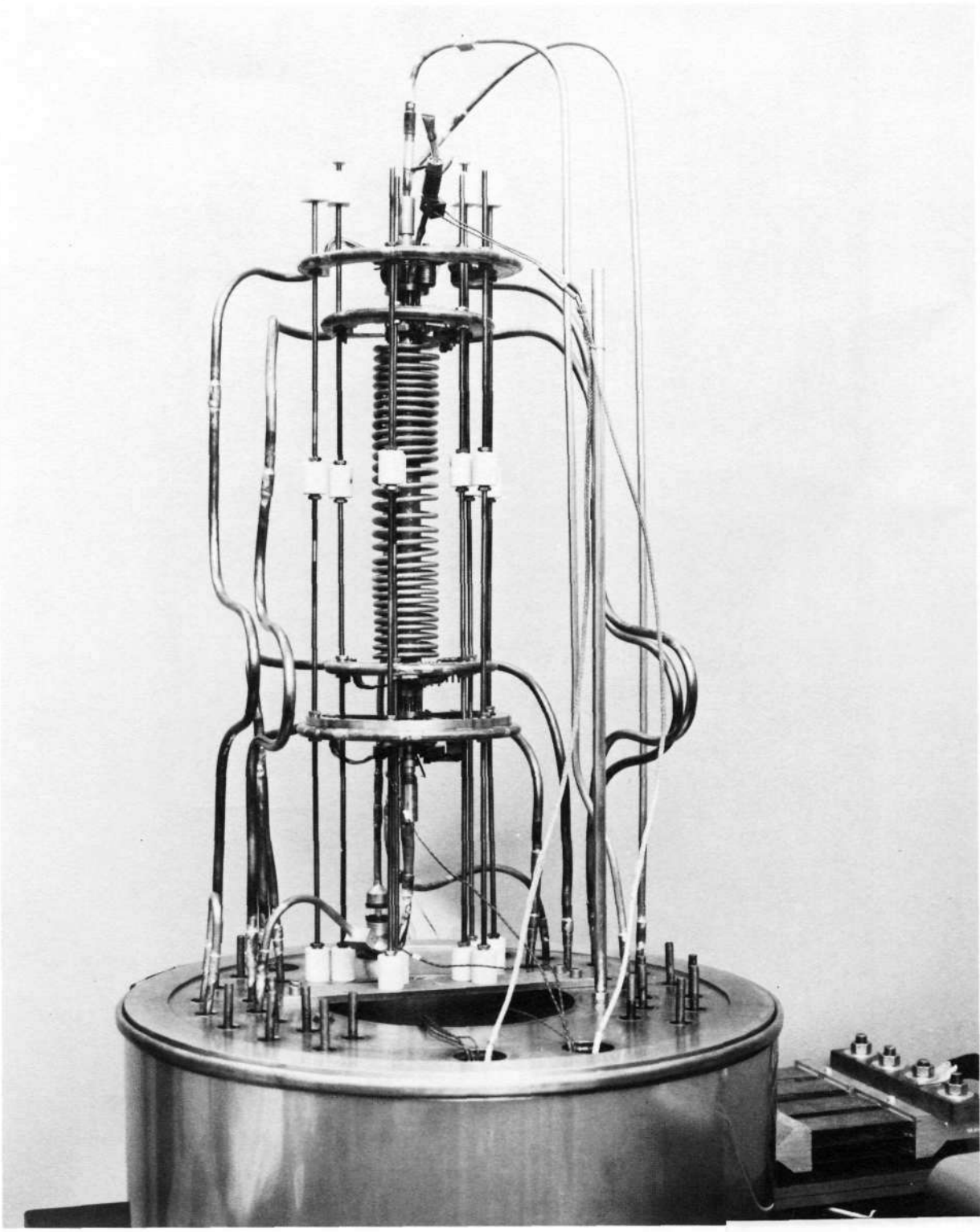

NOT REPRODUCIBLE

Fig. 2. Converter on test stand

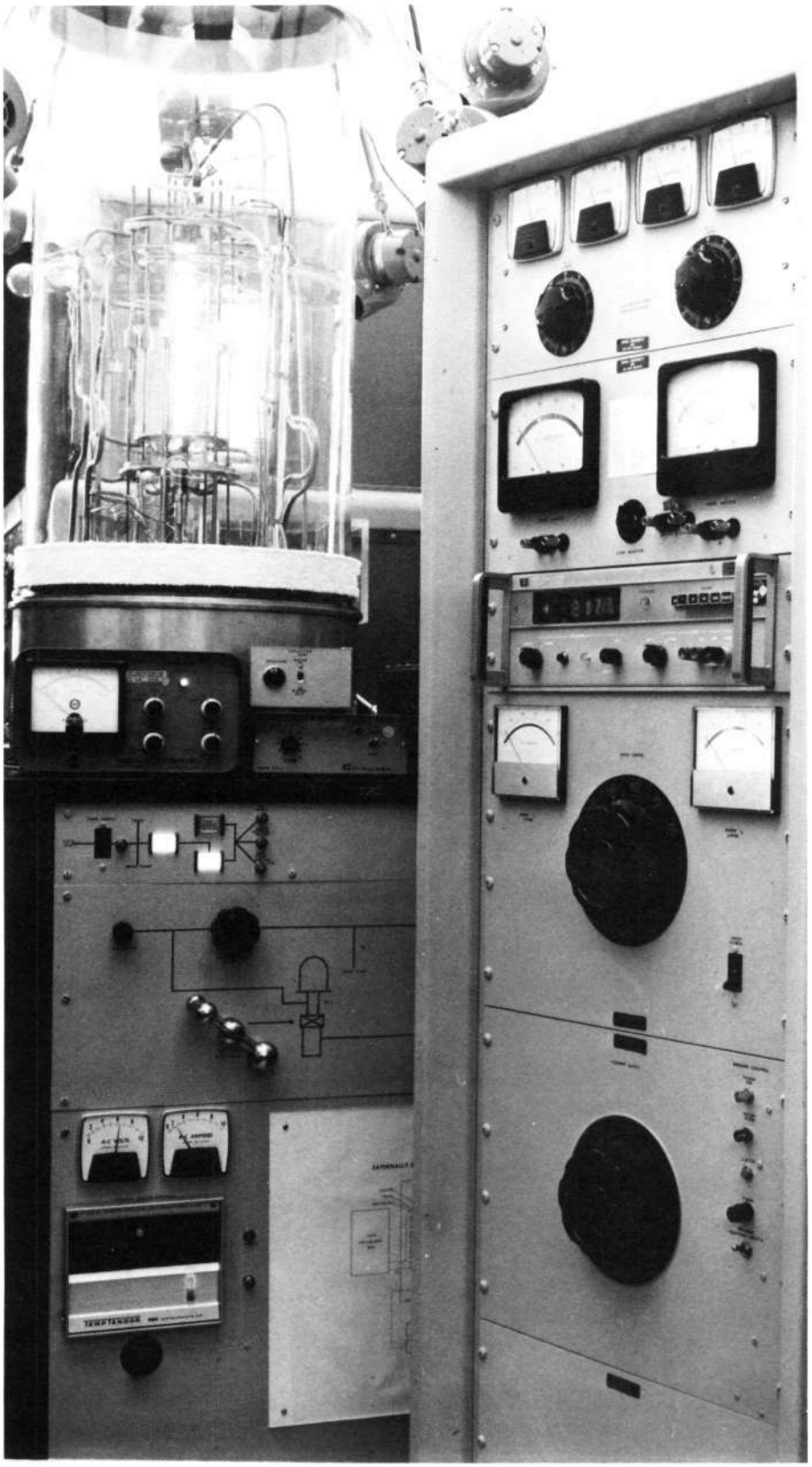

Fig. 3. Test setup

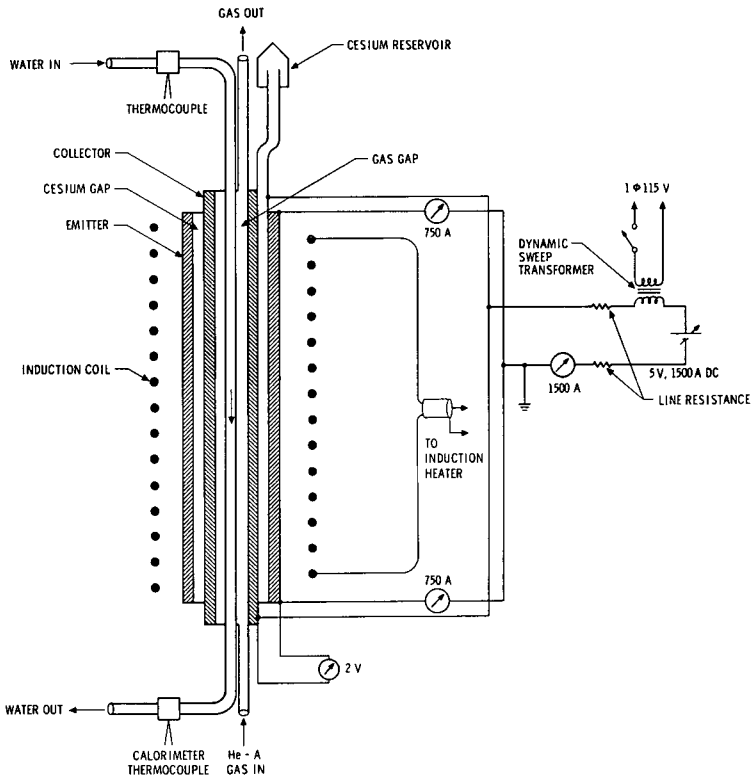

Fig. 4. Schematic diagram of test circuit

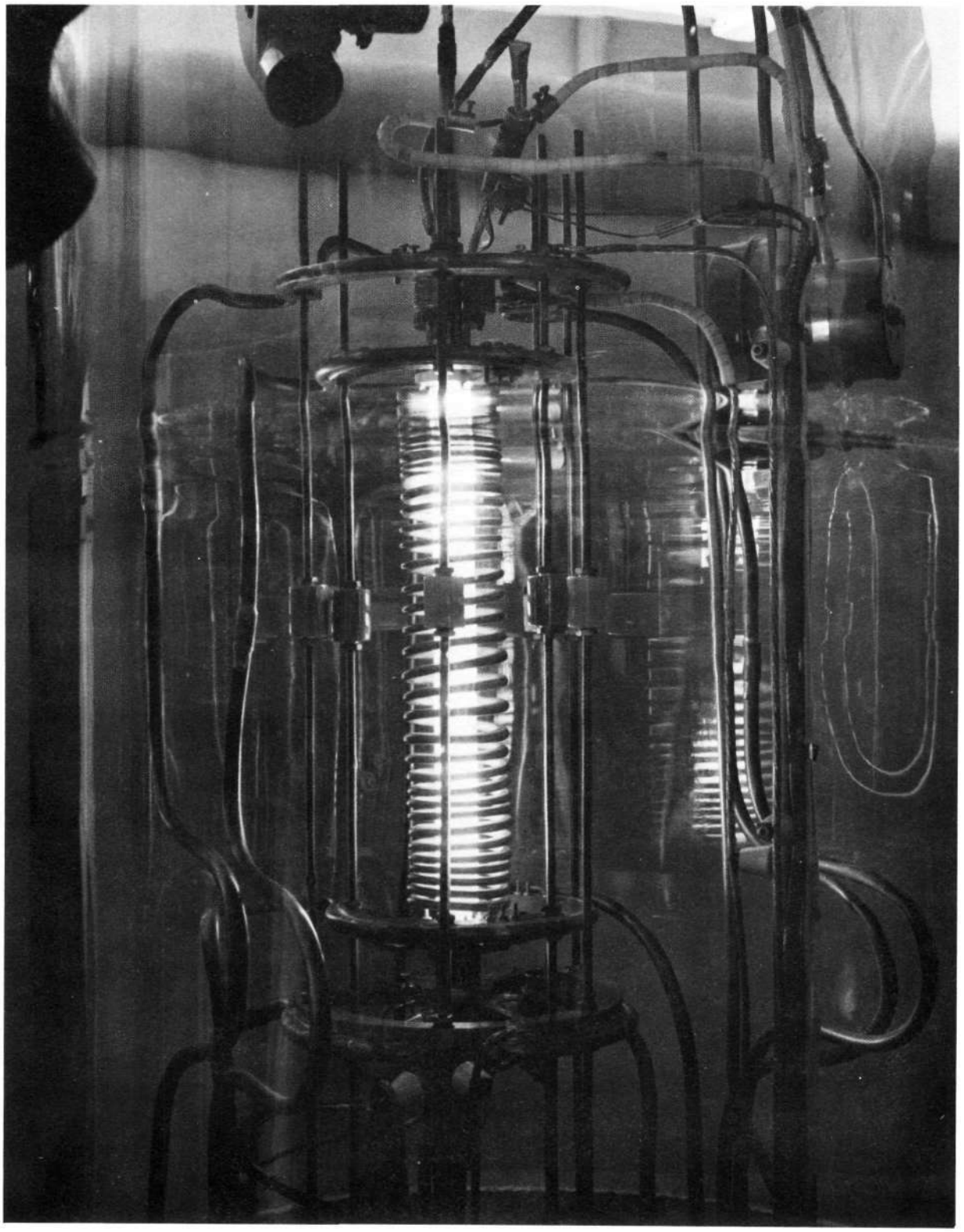

Fig. 5. Induction-heated converter

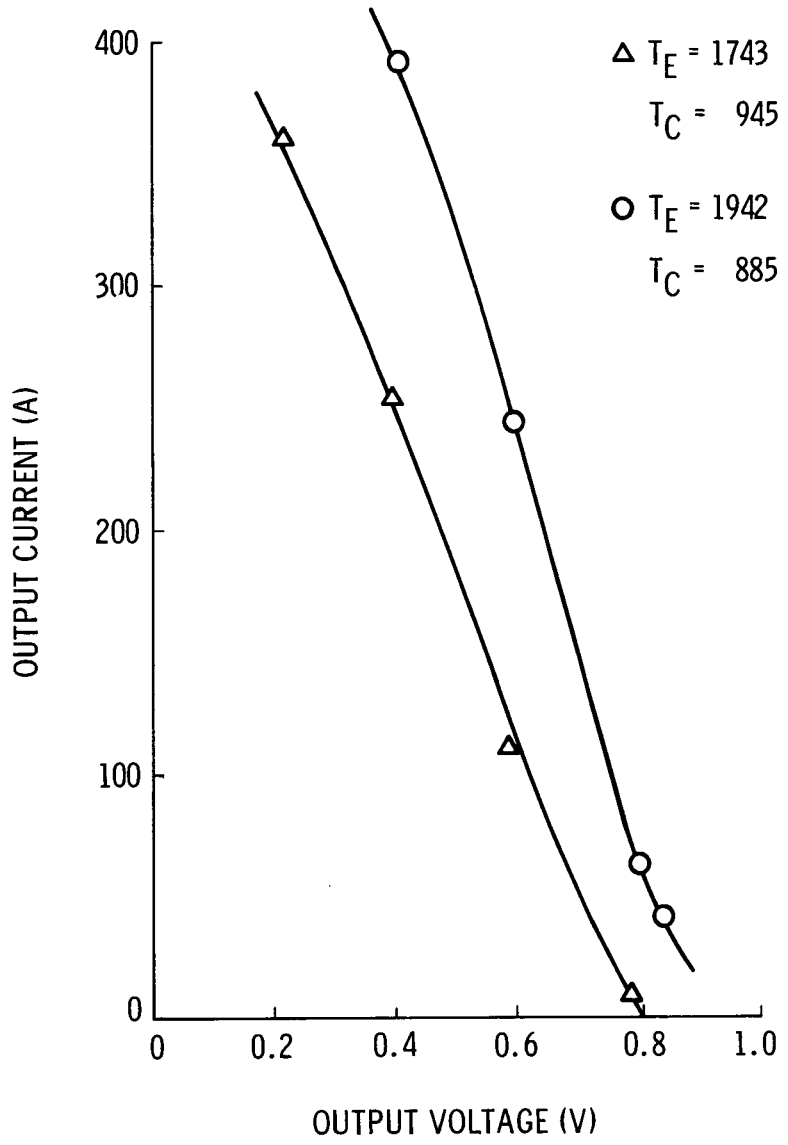

Fig. 6. Static volt-ampere curves, T_E = 1743 and 1946 K

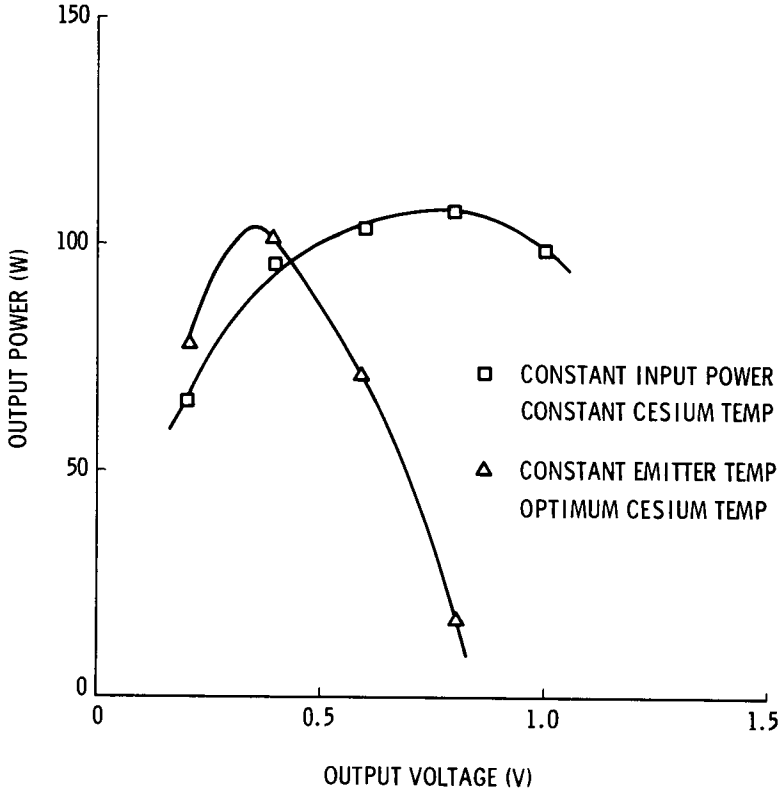

Fig. 7. Output power versus output voltage

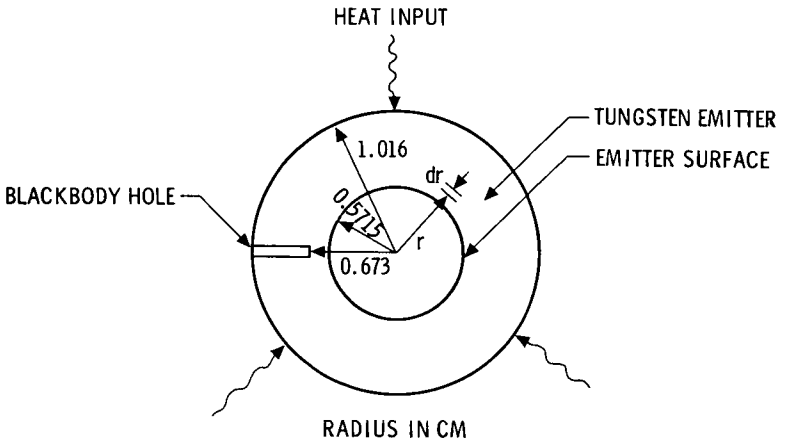

Fig. 8. Emitter cross section

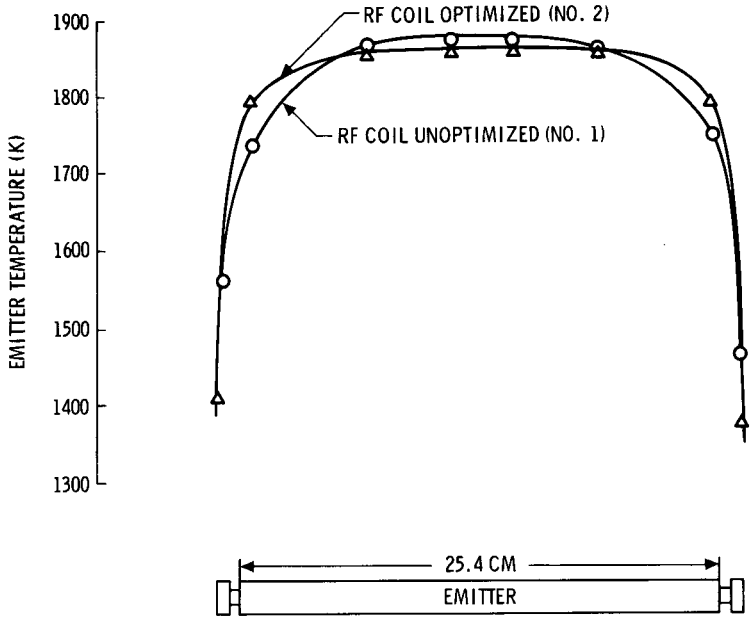

Fig. 9. Emitter temperature distribution

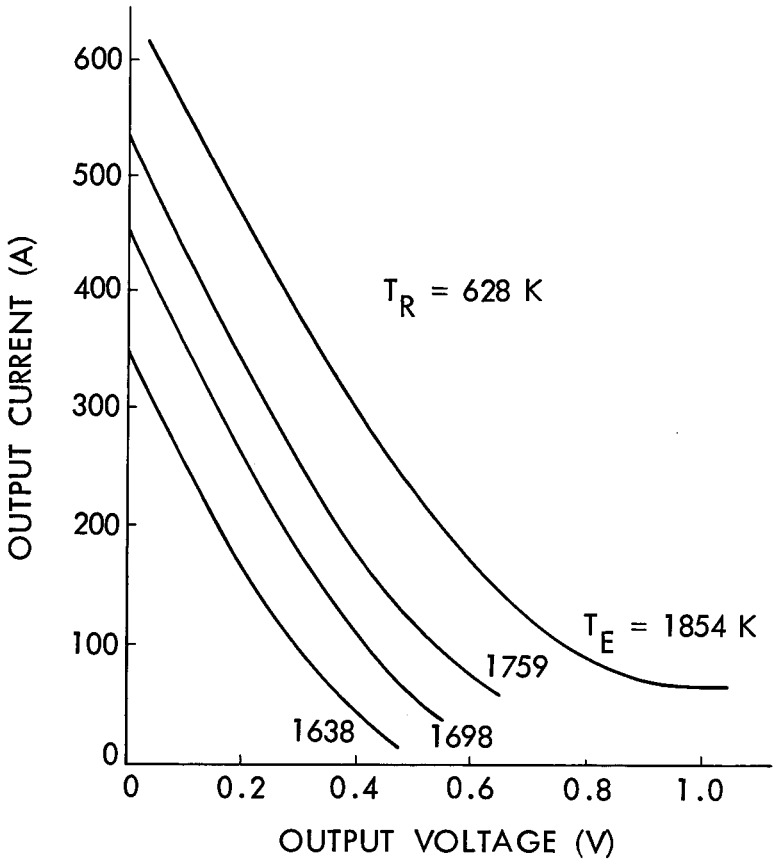

Fig. 10. Dynamic volt-ampere curves, T_E variable, T_R = 628 K

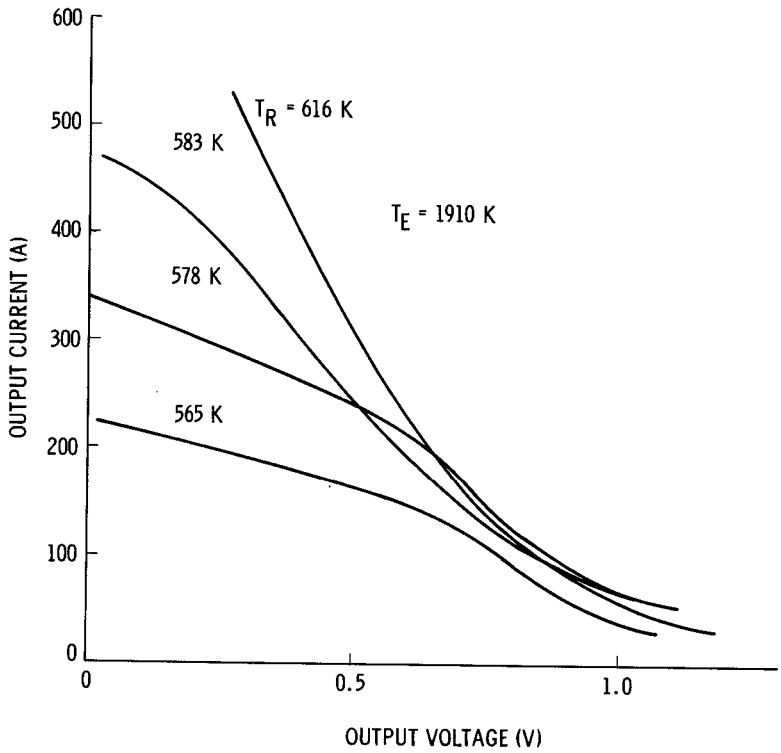

Fig. 11. Dynamic volt-ampere curves, T_R variable, T_E = 1910 K

REFERENCES

1. Ernst, D. M., "Design, Fabrication, and Testing of Externally Configured Thermionic Diodes," IEEE Conference Record of 1970 Thermionic Conversion Specialist Conference, Miami Beach, Fla., pp. 533-538, Oct. 1970.

2. Rouklove, P., and Shimada, K., Evaluation of Nuclear Thermionic Converters, JPL Internal Document No. 701-85, pp. 10-12, Jet Propulsion Laboratory, Pasadena, Calif., June 1970.

NASA — JPL — Coml., L.A., Calif.